The 4th International Symposium on More Electric Aircraft Technology (MEA 2017)

8–9 November 2017

Spectral analysis of a SVPWM modulated matrix converter based on 3D Fourier integral

Qiu Lin[1], Xu Lie[2], Li Yongdong[2], Huang Xiaoyan[1], Fang Youtong[1]

[1]*Electrical Engineering department, Zhejaing University, Xihu District, Hangzhou, People's Republic of China*
[2]*Electrical Engineering department, Tsinghua University, Haidian District, Beijing, People's Republic of China*
E-mail: qiu_lin@zju.edu.cn

Published in *The Journal of Engineering*; Received on 10th January 2018; Accepted on 17th January 2018

Abstract: Matrix converter (MC) is a typical high-power-density converter used in more electric aircraft, in which MC can be used as electric de-icer converter and generation starter converter; this study proposes an analytical spectral calculation method based on three-dimensional (3D) Fourier integral to obtain accurate spectra of both output voltage and input current of a space vector pulse width modulation (SVPWM) MC. The MC is a direct AC–AC power converter without an intermediate DC link; three-phase output is synthesised by three-phase input through nine bidirectional switches. At present, there is no such research on spectral analysis for MC space vector modulation. This study focuses on spectral calculation, by the adoption of 3D Fourier integral, spectral of bidirectional switch duty cycle function, output voltage and input current can be achieved. When analytic spectral solution is obtained, the correspondence between SVPWM and harmonic components is established. Simulation and experimental results are given to demonstrate the theoretical work.

1 Introduction

Matrix converter (MC) offers many advantages compared to traditional converter topologies (shown in Fig. 1), including unity input power factor, bi-directional power flow, improved input current harmonics, compact design and high power density without large energy storage elements [1–5]. The above advantages make the MC topology suitable for high power density application area; MC can be modulated through many strategies, such as Venturini, modified Venturini, space vector pulse width modulation (SVPWM) and so on. Among which SVPWM is the most popular method [6, 7], so far no research is done about the analytical spectral calculation process of SVPWM modulated MC.

The analytical spectral calculation is of significance since:

(i) Analytical result achieved is timesaving; no time-domain simulation is needed.
(ii) Analytical result can avoid error caused by truncation, limited cycle and so on.
(iii) Analytical result can easily guide the following harmonic suppression methods.

2 Spectral analysis of SVPWM modulated MC

The wide-use implement method of MC SVPWM is though look-up table, after sampling input voltage and direction of output current, space vector alone with its operation time in both diagrams can be achieved by naming output voltage (amplitude and direction) and input current (only direction) (Fig. 2).

Duty calculation of different space vectors is shown in (1)–(4), vectors I and II, vectors III and IV have the same direction in voltage diagram while vectors I and III, vectors II and IV are synclastic in current diagram

$$d_{\mathrm{I}} = \frac{2m_d}{\sqrt{3}} \frac{\cos\left(\tilde{\alpha} - (\pi/3)\right)\cos\left(\tilde{\beta} - (\pi/3)\right)}{\cos\delta} \tag{1}$$

$$d_{\mathrm{II}} = \frac{2m_d}{\sqrt{3}} \frac{\cos\left(\tilde{\alpha} - (\pi/3)\right)\cos\left(\tilde{\beta} + (\pi/3)\right)}{\cos\delta} \tag{2}$$

$$d_{\mathrm{III}} = \frac{2m_d}{\sqrt{3}} \frac{\cos\left(\tilde{\alpha} + (\pi/3)\right)\cos\left(\tilde{\beta} - (\pi/3)\right)}{\cos\delta} \tag{3}$$

$$d_{\mathrm{IV}} = \frac{2m_d}{\sqrt{3}} \frac{\cos\left(\tilde{\alpha} + (\pi/3)\right)\cos\left(\tilde{\beta} + (\pi/3)\right)}{\cos\delta} \tag{4}$$

2.1 Carrier wave equivalent SVPWM and three-dimensional (3D) Fourier integral theory

Zero vector is used to fill the gap in order to maintain the constant switching cycle

$$\begin{aligned} d_0 &= 1 - d_{\mathrm{I}} - d_{\mathrm{II}} - d_{\mathrm{III}} - d_{\mathrm{IV}} \\ &= 1 - \frac{2}{\sqrt{3}} m_d \frac{\cos(\tilde{\alpha})\cos(\tilde{\beta})}{\cos\delta} = \sum_{i=1}^{3} d_{0i} \end{aligned} \tag{5}$$

The look-up table is complicated in the process of analytical calculation, note that SVPWM is described based on input line voltage, carrier-based modulation methods which is equivalent to SVPWM should be achieved first, after enumerating different section conditions, Fig. 3 is summarised as follows.

Different input current sections (defined by *ki*) and different output voltage sections (defined by *kv*) lead to different duty cycle calculation and different input voltage sequence. According

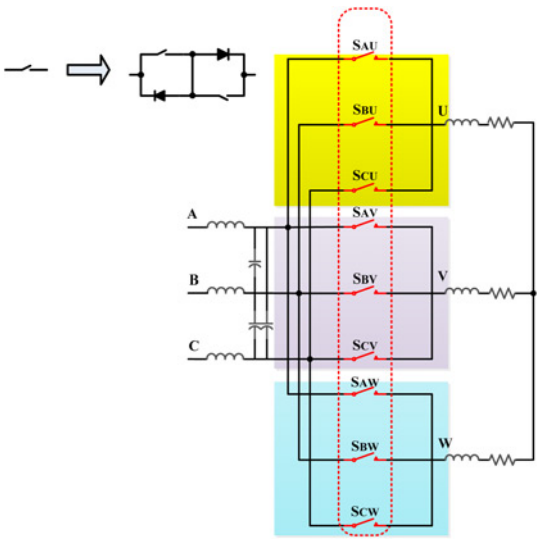

Fig. 1 *MC topology*

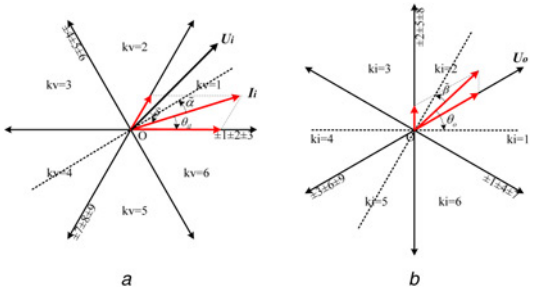

Fig. 2 *Space vector diagram of SVPWM modulated MC*
a Output voltage diagram
b Input current diagram

to input voltage sequence, define U_{01}, U_{02}, U_{03} in order, the correspondence of input voltage is shown in Table 1.

After summarising duty cycle calculation law in all input and output situations, carrier-based modulation can be achieved by adopting dual reference wave modulation process. The single and double side carrier-based wave is shown as follows (Fig. 4):

$$\begin{cases} c_{2-\text{side}}(x) = \dfrac{1}{\pi}\arccos(\cos x) \\ c_{1-\text{side}}(x) = \dfrac{1}{2\pi}\arccos(\cos 2x) \end{cases} \tag{6}$$

After duty-cycle calculation, MC SVPWM procedure will transform to carrier-based described form.

The triplet Fourier decomposition of a three-variable periodic function is shown below:

$$\begin{cases} f(x,y,z) = \displaystyle\sum_{k=-\infty}^{+\infty}\sum_{m=-\infty}^{+\infty}\sum_{n=-\infty}^{+\infty} F_{kmn}\mathrm{e}^{\mathrm{j}(kx+my+nz)} \\ F_{kmn} = \dfrac{1}{8\pi^3}\displaystyle\int_{-\pi}^{\pi}\int_{-\pi}^{\pi}\int_{-\pi}^{\pi} f(x,y,z)\mathrm{e}^{-\mathrm{j}(kx+my+nz)}\mathrm{d}x\mathrm{d}y\mathrm{d}z \end{cases} \tag{7}$$

In MC, these three variables are carrier phase angle, input phase angle, output phase angle, respectively; these variables should meet the requirement of independent, periodic (2π) and ergodic

$$\begin{cases} x = \omega_c t \\ y = \omega_{\text{in}} t + \theta_A \\ z = \omega_{\text{out}} t + \theta_B \end{cases} \tag{8}$$

2.2 Spectral analysis of SVPWM modulated MC

For SVPWM, different input current sections and different output voltage sections lead to different duty cycle calculation and different input voltage sequence. For three output phase, define *H*, *M*, *L* in order according to the operation duty cycle of U_{02}, which is summarised in Table 2; for example, when $kv = ki = 1$, *H*, *M*, *L* means output phase *U*, *V*, *W*, respectively.

With U_{01}, U_{02}, U_{03} defined in Table 1, spectrum of bi-direction switches is calculated as follows: (see (9)) (see (10))
$H_{U_{03}H}(k, m, n)$ is the spectrum of switch that connects output phase *H* (namely *U* when $kv = ki = 1$) and input phase U_{03} (namely *B* when

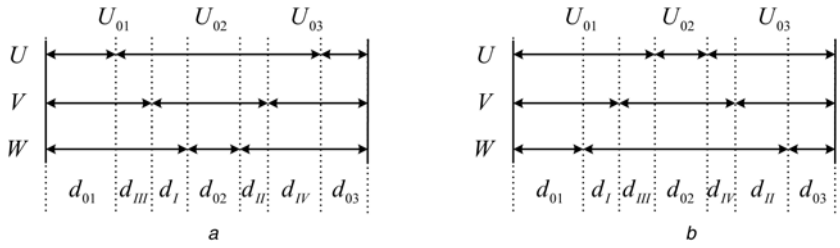

Fig. 3 *Parameter relationship in SVPWM modulated MC*
a $kv + ki$ equal even number
b $kv + ki$ equal odd number

$$\begin{cases} H_{U_{01}H}(k,m,n) = \int_{(kv-1)\pi/3}^{(kv-1)\pi/3+\pi/3}\int_{(ki-1)\pi/3-\pi/6}^{(ki-1)\pi/3+\pi/6-\pi}\int_{-\pi}^{-\pi} \mathrm{e}^{-\mathrm{j}(kx_c+mx_A+nx_B)}\mathrm{d}x_C\mathrm{d}x_A\mathrm{d}x_B \\ H_{U_{01}M}(k,m,n) = \int_{(kv-1)\pi/3}^{(kv-1)\pi/3+\pi/3}\int_{(ki-1)\pi/3-\pi/6-\pi}^{(ki-1)\pi/3+\pi/6-\pi}\int_{-\pi d_{\text{III}}}^{+\pi d_{\text{III}}} \mathrm{e}^{-\mathrm{j}(kx_c+mx_A+nx_B)}\mathrm{d}x_C\mathrm{d}x_A\mathrm{d}x_B \\ H_{U_{01}L}(k,m,n) = \int_{(kv-1)\pi/3}^{(kv-1)\pi/3+\pi/3}\int_{(ki-1)\pi/3-\pi/6-\pi}^{(ki-1)\pi/3+\pi/6-\pi}\int_{-\pi(d_I+d_{\text{III}})}^{+\pi(d_I+d_{\text{III}})} \mathrm{e}^{-\mathrm{j}(kx_c+mx_A+nx_B)}\mathrm{d}x_C\mathrm{d}x_A\mathrm{d}x_B \end{cases} \tag{9}$$

$$\begin{cases} H_{U_{03}H}(k,m,n) = \int_{(kv-1)\pi/3}^{(kv-1)\pi/3+\pi/3}\int_{(ki-1)\pi/3-\pi/6}^{(ki-1)\pi/3+\pi/6}\int_{\pi}^{\pi} \mathrm{e}^{-\mathrm{j}(kx_c+mx_A+nx_B)}\mathrm{d}x_C\mathrm{d}x_A\mathrm{d}x_B \\ H_{U_{03}M}(k,m,n) = \int_{(kv-1)\pi/3}^{(kv-1)\pi/3+\pi/3}\int_{(ki-1)\pi/3-\pi/6}^{(ki-1)\pi/3+\pi/6}\int_{-\pi d_{\text{IV}}}^{+\pi d_{\text{IV}}} \mathrm{e}^{-\mathrm{j}(kx_c+mx_A+nx_B)}\mathrm{d}x_C\mathrm{d}x_A\mathrm{d}x_B \\ H_{U_{03}L}(k,m,n) = \int_{(kv-1)\pi/3}^{(kv-1)\pi/3+\pi/3}\int_{(ki-1)\pi/3-\pi/6}^{(ki-1)\pi/3+\pi/6}\int_{-\pi(d_{\text{II}}+d_{\text{IV}})}^{\pi(d_{\text{II}}+d_{\text{IV}})} \mathrm{e}^{-\mathrm{j}(kx_c+mx_A+nx_B)}\mathrm{d}x_C\mathrm{d}x_A\mathrm{d}x_B \end{cases} \tag{10}$$

Table 1 Correspondence of input voltage and different sections

	U_{01}	U_{02}	U_{03}
$ki = 1, 4$	V_C	V_A	V_B
$ki = 2, 5$	V_B	V_C	V_A
$ki = 3, 6$	V_A	V_B	V_C

$kv = ki = 1$). After $H_{U_{03}H}(k, m, n)$ and $H_{U_{03}H}(k, m, n)$ is calculated, $H_{U_{02}H}(k, m, n)$ is obtained with the following equation:

$$\begin{cases} H_{U_{02}H}(k, m, n) = \Delta - H_{U_{01}H}(k, m, n) - H_{U_{03}H}(k, m, n) \\ H_{U_{02}M}(k, m, n) = \Delta - H_{U_{01}M}(k, m, n) - H_{U_{03}M}(k, m, n) \\ H_{U_{02}L}(k, m, n) = \Delta - H_{U_{01}L}(k, m, n) - H_{U_{03}L}(k, m, n) \end{cases} \quad (11)$$

Where Δ is described in the following equation:

$$\Delta = \int_{(kv-1)\pi/3}^{(kv-1)\pi/3+\pi/3} \int_{(ki-1)\pi/3-\pi/6}^{(ki-1)\pi/3+\pi/6} \int_{-\pi}^{\pi} \mathrm{e}^{-\mathrm{j}(kx_c+mx_A+nx_B)} \mathrm{d}x_C \mathrm{d}x_A \mathrm{d}x_B \quad (12)$$

Spectral of a typical bidirectional switch (duty cycle function of switch that connects input phase q and output phase p) is an accumulation of all possible fast Fourier transform (FFT) coefficients (including k, m and n)

$$H_{qb}(\omega) = \sum_{k,m,n=-\infty}^{\infty} H_{\mathrm{XX}}(k, m, n)\delta(\omega - (k\omega_{\mathrm{c}} + m\omega_{\mathrm{in}} + n\omega_{\mathrm{out}})) \quad (13)$$

Assuming ideal input situation, input voltage contains input frequency ω_i only

$$V_{\mathrm{in}(q)}(\omega) = \frac{V_i}{2}\left[\mathrm{e}^{-\mathrm{j}(q-1)(2\pi/3)}\delta(\omega - \omega_i) + \mathrm{e}^{\mathrm{j}(q-1)(2\pi/3)}\delta(\omega + \omega_i)\right] \quad (14)$$

Thus, from (9)–(12), spectra of output voltage and input current can be calculated as follows:

$$V_{o(p)}(\omega) = \int_{-\infty}^{\infty} H_{qp}(\gamma)V_{\mathrm{in}(q)}(\omega - \gamma)\,\mathrm{d}\gamma = \frac{V_i}{2}\sum_{q=1}^{3}\left[H_{qp}(\omega - \omega_i)\mathrm{e}^{-\mathrm{j}(q-1)(2\pi/3)} + H_{qp}(\omega + \omega_i)\mathrm{e}^{\mathrm{j}(q-1)(2\pi/3)}\right] \quad (15)$$

$$I_{\mathrm{in}}(q)(\omega) = \int_{-\infty}^{\infty} H_{qp}(\gamma)I_p(\omega - \gamma)\,\mathrm{d}\gamma = \frac{I_{\mathrm{out}}}{2}\sum_{p=1}^{3}\left[H_{qp}(\omega - \omega_o)\mathrm{e}^{-\mathrm{j}(p-1)(2\pi/3)} + H_{qp}(\omega + \omega_o)\mathrm{e}^{\mathrm{j}(p-1)(2\pi/3)}\right] \quad (16)$$

Table 2 Correspondence of output phase and different sections

	$ki = 1, 3, 5$	$ki = 2, 4, 6$
$kv = 1$	U, V, W	W, V, U
$kv = 2$	V, U, W	W, U, V
$kv = 3$	V, W, U	U, W, V
$kv = 4$	W, V, U	U, V, W
$kv = 5$	W, U, V	V, U, W
$kv = 6$	U, W, V	V, W, U

Considering the rotation transformation character of different sections (including voltage and current), all other sections can transform to a situation that $kv = ki = 1$ by multiplying $\mathrm{e}^{-\mathrm{j}[n(kv-1)(\pi/3)+(\pi/6)n+m(ki-1)(\pi/3)]}$ in frequency domain

$$\begin{cases} x'_A = x_A - (ki - 1)\dfrac{\pi}{3} \\ x'_B = x_B - (kv - 1)\dfrac{\pi}{3} - \dfrac{\pi}{6} \end{cases} \quad (17)$$

Take duty calculation d_{II} as example, spectrum can be achieved by (18) and (19), phase swift parameters are shown in Table 3, when

Table 3 Correspondence of phase swift and different duty cycle

	d_{I}	d_{II}	d_{III}	d_{IV}	$d_{\mathrm{I}} + d_{\mathrm{III}}$	$d_{\mathrm{II}} + d_{\mathrm{IV}}$
θ_1	$-\frac{1}{3}\pi$	$\frac{1}{3}\pi$	$-\frac{1}{3}\pi$	$\frac{1}{3}\pi$	$-\frac{1}{3}\pi$	$\frac{1}{3}\pi$
θ_2	$-\frac{2}{3}\pi$	$-\frac{1}{3}\pi$	$\frac{1}{3}\pi$	$\frac{2}{3}\pi$	0	0

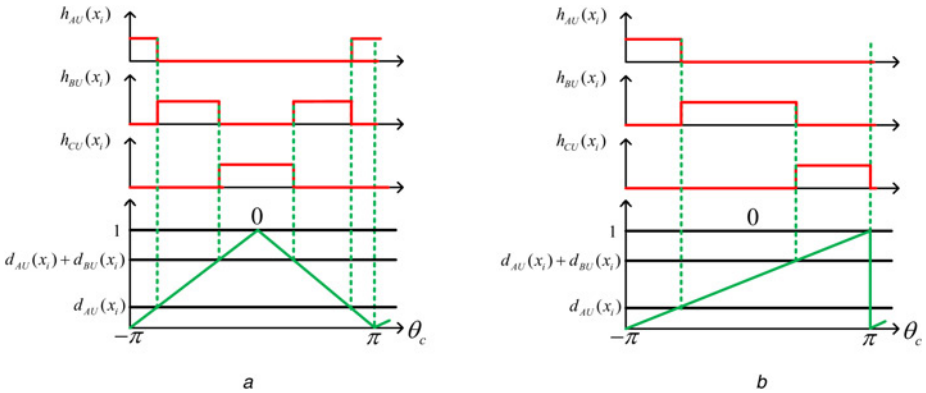

Fig. 4 *Dual reference wave modulation process*
a Double-side modulation
b Single-side modulation

doi: 10.1049/joe.2018.0060

Table 4 Simulation and experimental parameters

Simulation parameters	Value	Comment
input phase voltage	100 V	three phase
input frequency	50 Hz	—
reference output voltage	40 V	40% modulation index
reference output frequency	70 Hz	—
load	10 mH + 20Ω	three phase RL load
switching frequency	2 kHz	—
IGBT turn on delay	17 ns	Infineon bi-directional IGBT module FF200R12KT3_E
IGBT turn off delay	45 ns	—

$k=0$, (9) and (10) can be deduced to the following equations:

$$f_{\mathrm{II}} = \int_{-\pi/6}^{\pi/6}\int_{-\pi/6}^{\pi/6} (2\pi d_{\mathrm{II}})\mathrm{e}^{-\mathrm{j}(mx'_A+nx'_B)}\mathrm{d}x'_A\mathrm{d}x'_B \tag{18}$$

$$f_{\mathrm{II}} = \frac{4\pi m_d}{\sqrt{3}\cos\delta}\int_{-\pi/6}^{\pi/6}\int_{-\pi/6}^{\pi/6} \cos\left(x'_A+\theta_1\right)\ldots \cos\left(x'_B+\theta_2\right)\mathrm{e}^{-\mathrm{j}(mx'_A+nx'_B)}\mathrm{d}x'_A\mathrm{d}x'_B \tag{19}$$

When $k=0$, $f_{1\mathrm{I}}$ can separate into two different independent integrals

$$\begin{aligned} f_{\mathrm{II}} &= 4\pi C g_1 g_2 \\ &= 4\pi C\int_{-\pi/6}^{\pi/6} \cos\left(x'_A+\theta_1\right)\mathrm{e}^{-\mathrm{j}mx'_A}\mathrm{d}x'_A \\ &\quad \int_{-\pi/6}^{\pi/6} \cos\left(x'_B+\theta_2\right)\mathrm{e}^{-\mathrm{j}nx'_B}\mathrm{d}x'_B \end{aligned} \tag{20}$$

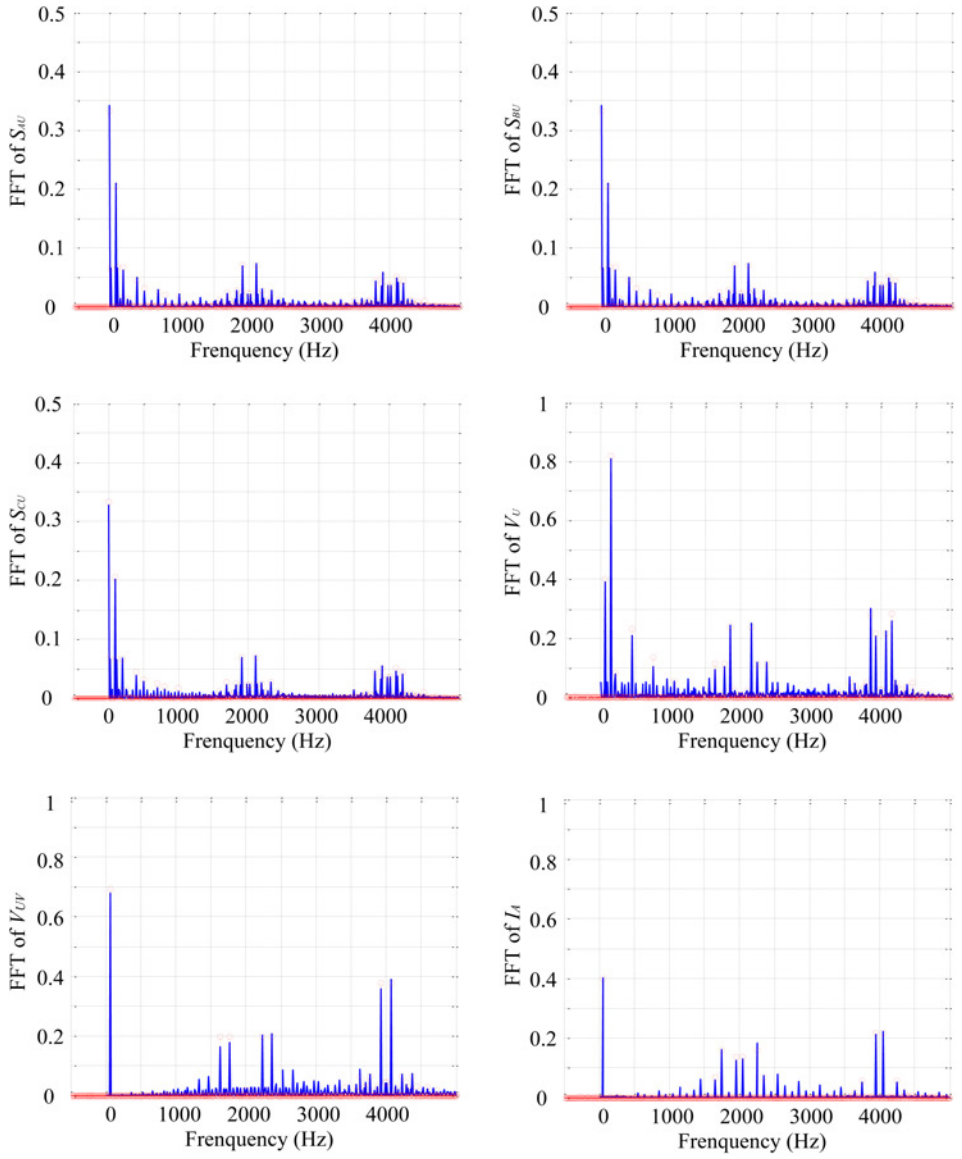

Fig. 5 *Analytical (red line) and simulation (blue line) results of SVPWM modulated MC*

Where function g_1 is expressed as follows:

$$g_1 = \int_{-\pi/6}^{\pi/6} \cos(x'_A + \theta_1) e^{-jmx'_A} dx'_A = \frac{1}{2}\left(e^{j\theta_1} \int_{-\pi/6}^{\pi/6} e^{j(1-m)x'_A} dx'_A + e^{-j\theta_1} \int_{-\pi/6}^{\pi/6} e^{-j(1+m)x'_A} dx'_A\right) \quad (21)$$

When k equals non-zero

$$f_{II} = \int_{-\pi/6}^{\pi/6} \int_{-\pi/6}^{\pi/6} e^{-jk\pi C\left[\begin{array}{l}\cos(x'_A + x'_B + \theta_1 + \theta_2)\ldots \\ +\cos(x'_A - x'_B + \theta_1 - \theta_2)\end{array}\right]} e^{-j(mx'_A + nx'_B)} dx'_A dx'_B \quad (22)$$

Using Jacob expansion for simplification, thus (23) can be achieved

$$f_{II} = \sum_{s1=-\infty}^{\infty} \sum_{s2=-\infty}^{\infty} \int_{-\pi/6}^{\pi/6} \int_{-\pi/6}^{\pi/6} e^{j(s_1+s_2-m)x'_A} e^{j(s_1-s_2-n)x'_B} dx'_A dx'_B \quad (23)$$

3 Simulation and experimental results

To validate the theoretical findings, a MATLAB simulation is utilised. The condition of simulations is shown in Table 4, simulation results of output voltage in 40% modulation indexes are presented to validate the theoretical results. Finally, the experimental results from a small experimental rig are presented to validate the simulation results; the parameter used in experiment and simulation is same.

Fig. 5 shows the comparison of simulation (red line) and theoretical (red line) results, the differences may be due to four-step commutation, limited simulation cycle and so on. The FFT analysis of each waveform shows the similar results to the simulation. The 40% output voltage utilisation result in 0.4 (in p.u. value) in base value of output phase voltage and input phase current, 0.69 in output line-voltage value.

Figs. 6 and 7 give the corresponding experimental waveforms, Fig. 6*a* shows the overall picture of experimental prototype whose bi-directional switch realised by Infineon bi-directional IGBT FF200R12KT3_E. Fig. 6*b* describes the time-domain waveforms of voltage and current of input and output side; it can be seen that the loads current are controlled with the correct amplitude and frequency. The output line voltages are staircase waveforms and input current are sine wave as expected, Fig. 7 shows the

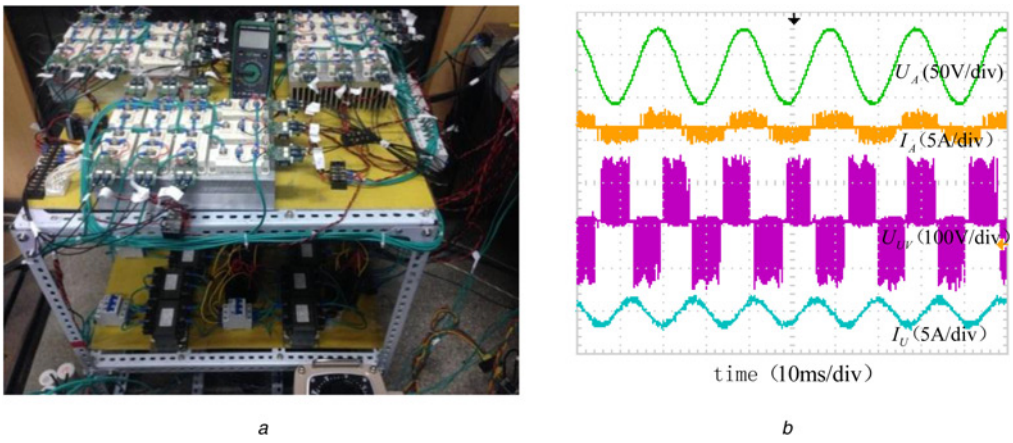

Fig. 6 *Experimental prototype and experiment results of SVPWM modulated MC*
a Experimental prototype for MC
b Time-domain experimental result

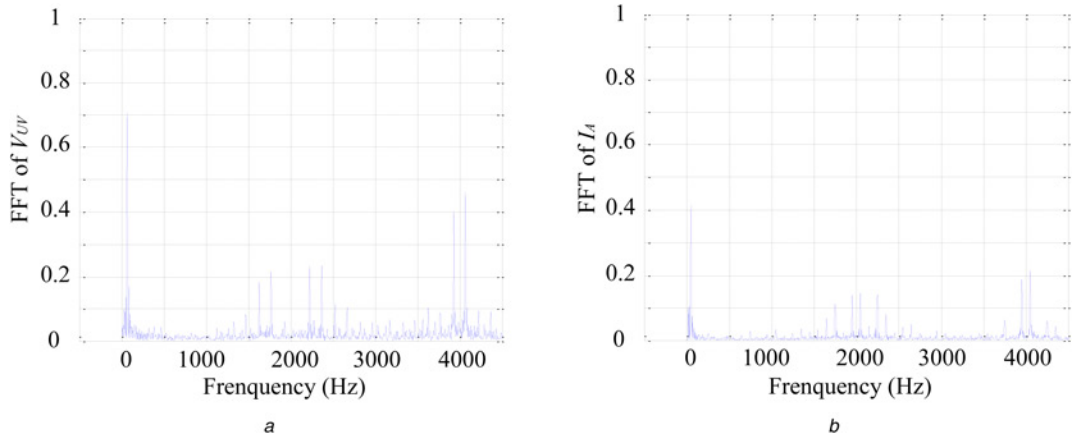

Fig. 7 *FFT of experimental waveforms*
a FFT of experimental output line voltage
b FFT of experimental input current

experimental result of Fig. 5, experiment results and simulation results are similar.

Comparing different switches (e.g. S_{AU}, S_{BU}, S_{CU}), baseband harmonics are similar in amplitude and position, which are located on $f_{in} \pm f_{out}$, $f_{in} \pm 3f_{out}$ and $f_{in} \pm 3f_{in}$ (namely 20, 100, 120, 160, 200 and 260 Hz in this situation). Consistent amplitude verifies the rotation characteristics described in Table 1. Since the offset effect between different sections, no harmonics exists when FFT variables $m+n$ equals even numbers.

4 Conclusion

Although SVPWM is the most popular modulation methods for MCs, no analytical spectral analysis exists for exact harmonic calculation and analyses; this paper proposes an analytical spectral calculation method based on 3D Fourier integral to obtain accurate spectra of both output voltage and input current. Simulation and experimental results are given to demonstrate the theoretical work.

5 Acknowledgments

My deepest gratitude goes first and foremost to Professor Li Yondong, my supervisor, for his constant encouragement and guidance. He has walked me through all the stages of the writing of this thesis. Also, I would like to express my heartfelt gratitude to Associate Professor Xu Lie, who led me into the world of Matrix converter.

6 References

[1] Inomata K., Hara H., Morimoto S., *ET AL.*: 'Enhanced fault ride through capability of matrix converter for wind power system'. The Thirty-Ninth Annual Conf. of the IEEE Industrial Electronics Society, 2013, pp. 4838–4843

[2] Inomata K., Hara H., Morimoto S., *ET AL.*: 'Application of modular matrix converter to wind turbine generator'. Int. Power Electronics Conf., 2014, pp. 1654–1659

[3] Yamamoto E., Hara H., Uchino T., *ET AL.*: 'Development of MCs and Its applications in industry [industry forum]', *IEEE Ind. Electron. Mag.*, 2011, **5**, (1), pp. 4–12

[4] Blaabjerg F., Casadei D., Klumpner C., *ET AL.*: 'Comparison of Two current modulation strategies for matrix converters under unbalanced input voltage conditions', *IEEE Trans. Ind. Electron.*, 2002, **49**, (2), pp. 289–296

[5] Casadei D., Serra G., Tani A.: 'Reduction of The input current harmonic content in matrix converters under input/output unbalance', *IEEE Trans. Ind. Electron.*, 1998, **45**, (3), pp. 401–411

[6] Accioly A.G.H., Bradaschia F, Cavalcanti M.C., *ET AL.*: 'A New general approach for modulation strategies in matrix converters'. IEEE Int. Symp. on Industrial Electronics, 2007, pp. 685–690

[7] Accioly A.G.H, Bradaschia F, Cavalcanti M.C., *ET AL.*: 'Generalized modulation strategy for matrix converters - part I'. IEEE Power Electronics Specialists Conf., 2007, pp. 646–652